Bandgap and exciton binding energies of hexagonal boron nitride probed by photocurrent excitation spectroscopy

T. C. Doan, J. Li, J. Y. Lin, and H. X. Jiang[a)]
Department of Electrical and Computer Engineering, Texas Tech University, Lubbock, Texas 79409, USA

Photocurrent excitation spectroscopy has been employed to probe the band structure and basic parameters of hexagonal boron nitride (*h*-BN) epilayers synthesized by metal-organic chemical vapor deposition. Bias dependent photocurrent excitation spectra clearly resolved the band-to-band, free exciton, and impurity bound exciton transitions. The energy bandgap (E_g), binding energy of free exciton (E_x), and binding energy of impurity bound exciton (E_{bx}) in *h*-BN have been directly obtained from the photocurrent spectral peak positions and comparison with the related photoluminescence emission peaks. The direct observation of the band-to-band transition suggests that *h*-BN is a semiconductor with a direct energy bandgap of $E_g = 6.42$ eV at room temperature. These results provide a more coherent picture regarding the fundamental parameters of this important emerging ultra-wide bandgap semiconductor. *Published by AIP Publishing.*
[http://dx.doi.org/10.1063/1.4963128]

Hexagonal boron nitride (*h*-BN) has recently attracted much interest due to its potential as a deep-ultraviolet (DUV) photonic material,[1–5] as an ideal material for the exploration of van der Waals heterostructures made layer by layer between *h*-BN/graphene related materials with new physics and applications,[6–8] and as a solid-state neutron detector material.[9–11] Previous studies have also revealed that *h*-BN epilayers exhibit extremely high optical absorption above bandgap ($\sim 7.5 \times 10^5$ cm^{-1}) and emission.[4,12–14] More recently, it was shown that by growing *h*-BN under high ammonia flow rates, nitrogen vacancy related emission peaks can be eliminated and consequently, epilayers exhibiting pure free exciton emission at low temperatures can be achieved.[15] However, fundamental parameters of *h*-BN remain to be probed. The energy bandgap (Eg) and the free exciton binding energy (E_x) of this material have been theoretically calculated[14,16–18] and experimentally determined to be near 6.5 and 0.7 eV, respectively.[19–23] The confirmation of these parameters by more direct experimental measurements is highly desirable. Also, there remains controversy regarding if *h*-BN is a direct or an indirect bandgap semiconductor. The realization of wafer-scale semiconducting *h*-BN epilayers with high crystalline and optical qualities has opened up opportunities for the exploration of the fundamental properties and emerging applications of this important material.

Photoluminescence (PL) emission spectroscopy has been widely utilized as one of the most effective methods to identify the fundamental bandgap and exciton binding energies in semiconductors. In wide bandgap semiconductors, the band-to-band transition with its energy peak position corresponding to the energy bandgap is often difficult to observe directly due to the dominance of the excitonic transitions. For instance, in GaN and AlN, the exciton binding energies can be determined either from the emission energy difference between the first excited state and the ground state or

from the thermal activation of the excitonic emission intensities.[24,25] Consequently, the energy bandgap of GaN or AlN can thus be deduced by knowing the spectral peak position of the excitonic transition and the binding energy of the free exciton. However, in *h*-BN, due to the exceptionally large exciton binding energy and exciton-phonon interaction, it is difficult to detect the thermal activation of the free excitonic transition or the first excited state of the free exciton. As a consequence, direct determination of the energy bandgap from the PL or optical absorption measurement is challenging. Previous photoconductivity and photoluminescence excitation spectroscopy measurements have provided a room temperature bandgap of *h*-BN of about 6.4 eV based on the observation of an optical absorption edge.[19,20] In this work, photocurrent excitation spectroscopy has been utilized as an alternative technique to directly probe the energy bandgap and exciton binding energies. The generation of photocurrent requires the excitation of the free charge carriers or excitons as well as charge carrier separation and collection under the aid of an electric field, and hence provides an avenue for the direct observation of the band-to-band and excitonic transition.

Epitaxial layers of *h*-BN employed in this study were synthesized by metal-organic chemical vapor deposition (MOCVD) using triethylboron (TEB) and ammonia (NH$_3$) as the precursors for B and N, respectively. Epilayers were grown on *c*-plane sapphire substrates at 1300 °C using hydrogen as a carrier gas. The surface roughness was probed by atomic force microscope (AFM) revealing a root mean square (RMS) of 0.2 nm in a scanning area of 1 μm × 1 μm. The PL spectroscopy system consists of a frequency quadrupled 100 femtosecond Ti: sapphire laser with excitation photon energy set around 6.28 eV and a monochromator (1.3 m). A single photon counting detection system in conjunction with a micro-channel-plate photo-multiplier tube was used to record PL spectra.[23–25] For the photocurrent excitation spectroscopy measurements, photodetectors based on a metal-semiconductor-metal (MSM) architecture with micro-strip

a)E-mail: hx.jiang@ttu.edu

109, 122101-1

interdigital fingers were fabricated from *h*-BN epilayers.[11] The photolithography technique was used to pattern the interdigital fingers on the surface of *h*-BN epilayers. Contacts consisting of bi-layers of Ti/Al (20 nm/30 nm) were deposited by e-beam evaporation for the application of bias voltages and the collection of the charge carriers (or photocurrent). A broad light source covering wavelength range between 170 and 2100 nm [model E-99 laser-driven light source (LDLS) by Energytiq] coupled with a triple grating monochromator (Pro 2300 I of Acton by Research Corporation Spectra) was used as a variable wavelength excitation source with an excitation spectral resolution of about 0.2 nm.

The basic layer structure of *h*-BN epilayers (30 nm in thickness) used in this study is shown in the inset of Fig. 1(a). The x-ray diffraction (XRD) θ-2θ scan shown in Fig. 1(a) is similar to those reported previously[4,13] and reveals that the BN films are single crystals of hexagonal phase.[26–28] Figure 1(b) shows an optical image of a fabricated MSM detector. The MSM detector has a device size of 0.5 mm × 0.5 mm with metal strips of 6 μm in width and spacing between the
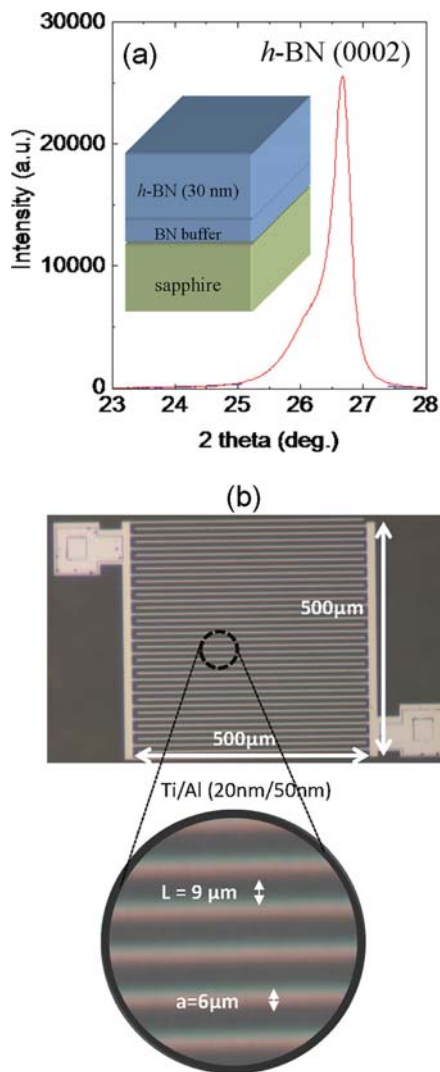
metal strips of 9 μm. Figure 2 shows the I–V characteristics of the dark (open squares) and photocurrent (open circles) of a *h*-BN MSM detector under the excitation of a broad spectrum light source. Both dark and photocurrent exhibit linear behavior. Under the photoexcitation, the conductivity of the *h*-BN epilayer is increased by a factor of approximately 10 due to an increase in the photo-excited free carrier concentration and reduced electrical resistivity.

Figure 3 shows the room temperature photocurrent excitation spectra of an *h*-BN epilayer measured at different bias voltages, V_b, from 1 to 100 V corresponding to applied electric fields of 1.1×10^3 V/cm to 1.1×10^5 V/cm. A photocurrent excitation spectrum effectively records the increase in the free carrier concentration (electrons and holes) due to photoexcitation and the peaks in these spectra form as a result of carriers/excitons making transitions from different energy levels or bands. For instance, the free exciton transition peak in a photocurrent spectrum is formed through the processes of resonant excitation of free excitons (absorbing photons with an energy equal to that of the free exciton transition) and subsequent dissociation of a fraction of excitons into free carriers in the presence of an applied electric field. The peak height increases with an increase of the applied voltage or electric field due to the fact that the process of breaking-up of free excitons as well the efficiency of charge collection is enhanced by an increase of the bias voltage or electric field. Transition peaks at 4.17, 5.39, 5.69, and 6.42 eV are clearly resolved in the photocurrent excitation spectra shown in Fig. 3. The 4.17 eV transition is due to the well-known donor-acceptor-pair (DAP) transition involving a nitrogen vacancy (V_N) donor with an energy level at about 0.1 eV, and a deep level acceptor possibly associated with the carbon impurity occupying the nitrogen site with an energy level of 2.3 eV.[29–32] The transition at 5.39 eV has been previously identified and is most likely due to another DAP transition involving the same shallow V_N donor and a deep acceptor with an energy level of about 1.1 eV.[15,31] The trend shown in Fig. 3 indicates that lower energy transition peaks require relatively higher bias voltages to observe. This is because an additional electric field is needed to further break-up the carriers or excitons bound to impurities into
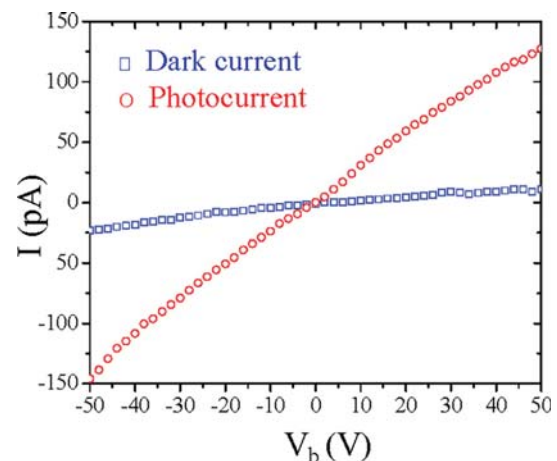

FIG. 1. (a) XRD θ-2θ scan of an *h*-BN epilayer grown by MOCVD. The inset shows the layer structure of *h*-BN epilayers used in this study. (b) Optical images of a fabricated detector used for measuring the photocurrent excitation spectra.

FIG. 2. I–V characteristics of dark (open squares) and photocurrent (open circles) under the illumination of a broad spectrum light source.
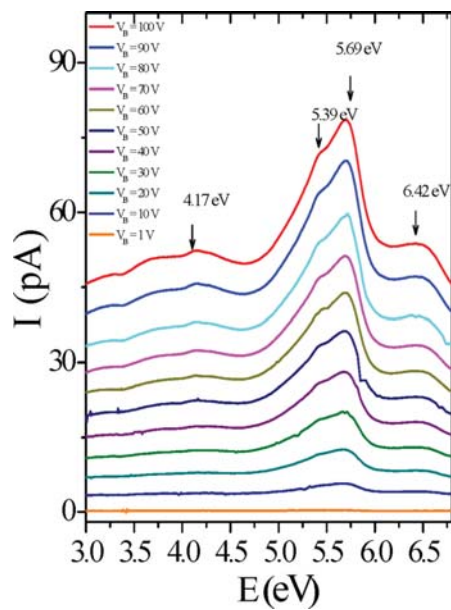
FIG. 3. Room temperature photocurrent excitation spectra of *h*-BN epilayers measured at different bias voltages (V$_b$).

free carriers. Consequently, the DAP transition at 4.17 eV is observable at highest V$_b$. It is interesting to note that high energy transition peaks at 5.69 eV and 6.42 eV are observable at a bias voltage as low as V$_b$ = 20 V.

Figure 4 plots the comparison between the photocurrent excitation and PL emission spectra of an *h*-BN epilayer. Figure 4(a) is the 300 K photocurrent excitation spectrum
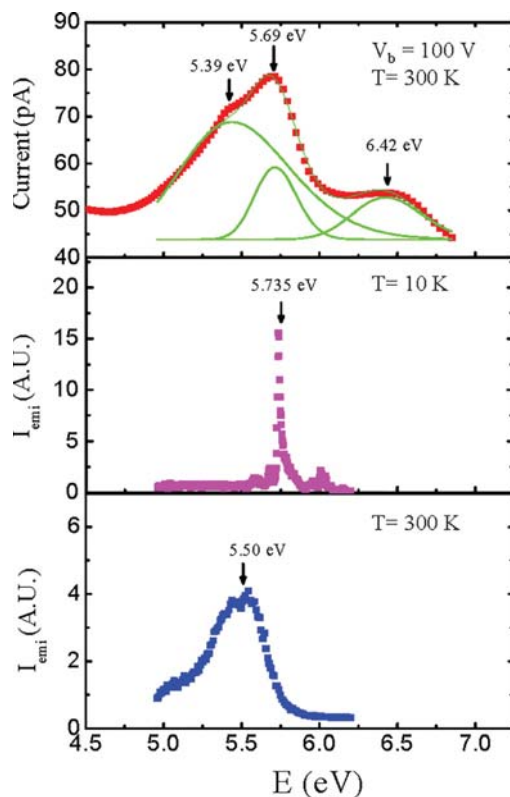

FIG. 4. Comparison of (a) photoexcitation spectrum obtained at 300 K and V$_b$ = 100 V, (b) free exciton PL spectrum obtained at 10 K, and (c) impurity bound exciton PL spectrum obtained at 300 K for an *h*-BN epilayer.

obtained at 100 V. Figure 4(b) shows the low temperature (10 K) PL spectrum which shows that the free exciton emission line near 5.735 eV is the dominant transition line,[15] whereas Fig. 4(c) is the PL emission spectrum obtained at 300 K where the dominant emission line near 5.5 eV is due to the recombination of an impurity bound exciton.[15] Comparing the results shown in Figs. 4(a) and 4(b), the transition at 5.69 eV observed in the photoexcitation spectrum in Fig. 4(a) can be attributed to the free exciton transition. The free exciton transition peak in the photocurrent excitation spectrum is quite broad. This may be partly due to a possible nonuniformity in the charge collection efficiency. Due to the specific interdigital finger contact architecture shown in Fig. 1(b), the electric field at the center of the detector is slightly higher than that near the edge, leading to a nonuniformity in the charge collection efficiency. Moreover, a spectral overlap with a possible peak associated with an impurity bound exciton transition near 5.5 eV appearing in the room temperature PL spectrum in Fig. 4(c), which is not resolved in the photocurrent excitation spectrum, could also contribute to the broadening of the 5.69 eV peak in the photocurrent excitation spectrum.

The most significant result is the observation of the 6.42 eV peak. This transition peak corresponds well with the previously observed optical absorption edge at around 6.4 eV (Refs. 19 and 20) and hence can be assigned to the direct band-to-band excitation in *h*-BN epilayers. The fact that this is the highest energy peak in the spectrum also suggests that the 6.42 eV line corresponds to the band-to-band transition. The direct observation of the band-to-band transition is not expected from PL emission spectra due to the exceptionally large exciton binding energy in *h*-BN (around 0.7 eV). With the direct observation of the band-to-band and exciton transition lines, important information regarding the band structure and basic parameters of *h*-BN can thus be obtained.

By attributing the 6.42 eV line to the band-to-band transition, we directly obtain the room temperature energy bandgap of *h*-BN: E$_g$ = 6.42 eV. This value is slightly smaller than the low temperature value of E$_g$ = 6.5 eV deduced indirectly from the temperature dependent exciton recombination lifetime in *h*-BN bulk crystals[23] and from the theoretical calculations.[16–18] The 80 meV difference may be accounted for by the energy gap variation with temperature from room to low temperatures.[33] If we ignore the temperature effect, the present results together with previous experimental studies[19,20,23] provide a bandgap value for *h*-BN in between 6.4 and 6.5 eV. The free exciton binding energy (E$_x$) can also be directly obtained from the energy separation between the band-to-band and the exciton transition peaks: E$_x$ = 6.42 eV − 5.69 eV = 0.73 eV. This value agrees very well with the value of 0.74 eV deduced from the temperature dependent exciton recombination lifetime in *h*-BN bulk crystals[23] and also with the theoretical calculations.[14,16–18] Furthermore, by comparing the results of Figs. 4(a) and 4(c), the binding energy of the impurity bound exciton can also be obtained: E$_{bx}$ = 5.69 eV − 5.5 eV ≈ 0.2 eV. This value again agrees well with the energy difference between the free and impurity bound exciton emission lines observed in *h*-BN bulk crystals[34] and epilayers.[15] Based on these results, we have constructed in Fig. 5, the energy band diagram for
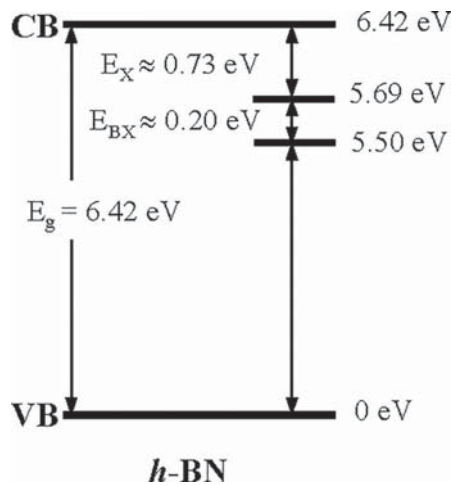
FIG. 5. Energy band diagram including the room temperature energy bandgap (E_g), binding energy of free exciton (E_x), and binding energy of impurity bound exciton (E_{bx}) in *h*-BN epilayers directly obtained from the photocurrent excitation spectra.

h-BN at room temperature, illustrating the energy bandgap (E_g), exciton binding energy (E_x), and binding energy of impurity bound exciton (E_{bx}). In constructing Fig. 5, we are not considering possible effects due to strain. Since MOCVD growth of *h*-BN is considered belonging to the class of van de Waals epitaxy, the possibility for the presence of strain and its effects on the optical and electrical properties of *h*-BN are unknown at this point.

The present results also have implications for understanding the nature of the energy bandgap of *h*-BN—direct vs. indirect, which is still very controversial at this stage. Most theoretical calculations[16–18] suggest an indirect bandgap, while many experiments have revealed evidence for a direct energy bandgap.[1–4,12–14] The direct observation of the band-to-band transition in the photocurrent excitation spectra with its spectral peak position corresponding well with the energy bandgap certainly implies that *h*-BN is a direct bandgap semiconductor. Otherwise, a phonon has to be involved to satisfy the conservation of both momentum and energy, leading to an immeasurable photocurrent. Moreover, the theoretically predicted indirect bandgap around 5.95 eV (Ref. 16) was not observed in the photocurrent excitation spectra shown in Fig. 3. In addition to the direct observation of the band-to-band transition reported here, all previous experimental results, including (a) the PL emission intensity of *h*-BN being two orders of magnitude larger than that of AlN,[4,14] (b) huge optical absorption coefficient in the order of 7.5×10^5/cm for above bandgap photons,[12,13] (c) lasing of *h*-BN under e-beam pumping[3] and (d) recent identification of only one direct intrinsic free exciton transition with all of its phonon modes being associated with the center of the Brillouin zone in *h*-BN bulk crystals[34] all support the view that *h*-BN is a direct bandgap semiconductor. An interesting remaining question is concerning the observation of exciton dissociation at an applied voltage as low as 20 V (corresponding to an electric field $\sim 2.2 \times 10^4$ V/cm), considering the very large exciton binding energy in *h*-BN. The exciton dissociation phenomenon seems to resemble the high efficiency of free charge carrier generation

in organic materials, in which excitons can dissociate via various mechanisms despite their huge binding energies (can be as large as >1 eV).[35] In *h*-BN, the presence of local fields induced by ionized defects (donors and acceptors) could also enhance the long-range exciton dissociation as in the case of organic solar cells.[35] Moreover, increased exciton recombination lifetime under an applied electric field could also enhance the dissociation of excitons. However, this phenomenon of high free charge carrier generation efficiency under a moderate applied electric field in h-BN remains to be understood.

In summary, photocurrent excitation spectroscopy has been utilized as an effective means to probe the fundamental band parameters of *h*-BN. Transitions corresponding to the direct band-to-band, free excitons, and impurity bound excitons have been directly observed. From the observed transition peak positons, the determination of the room temperature bandgap ($E_g \sim 6.42$ eV), binding energy of excitons ($E_x \sim 0.73$ eV), and binding energy of impurity bound excitons ($E_{bx} \sim 0.2$ eV) in *h*-BN has become straightforward. The determination of these fundamental parameters in *h*-BN is important for both the basic understanding as well as potential applications of this emerging ultra-high bandgap semiconductor.

[1]Y. Kubota, K. Watanabe, O. Tsuda, and T. Taniguchi, Science **317**, 932 (2007).
[2]K. Watanabe, T. Taniguchi, T. Niiyama, K. Miya, and M. Taniguchi, Nat. Photonics **3**, 591 (2009).
[3]K. Watanabe, T. Taniguchi, and H. Kanda, Nat. Mater. **3**, 404 (2004).
[4]R. Dahal, J. Li, S. Majety, B. N. Pantha, X. K. Cao, J. Y. Lin, and H. X. Jiang, Appl. Phys. Lett. **98**, 211110 (2011).
[5]S. Majety, J. Li, X. K. Cao, R. Dahal, B. N. Pantha, J. Y. Lin, and H. X. Jiang, Appl. Phys. Lett. **100**, 061121 (2012).
[6]A. K. Geim and I. V. Grigorieva, Nature **499**, 419 (2013).
[7]N. Alem, R. Erni, C. Kisielowski, M. D. Rossell, W. Gannett, and A. Zettl, Phys. Rev. B **80**, 155425 (2009).
[8]C. R. Dean, A. F. Young, I. Meric, C. Lee, L. Wang, S. Sorgenfrei, K. Watanabe, T. Taniguchi, P. Kim, K. L. Shepard, and J. Hone, Nat. Nanotechnol. **5**, 722 (2010).
[9]A. Maity, T. C. Doan, J. Li, J. Y. Lin, and H. X. Jiang, Appl. Phys. Lett. **109**, 072101 (2016).
[10]T. C. Doan, S. Majety, S. Grenadier, J. Li, J. Y. Lin, and H. X. Jiang, Nucl. Instrum. Methods Phys. Res. Sect. A **748**, 84 (2014).
[11]T. C. Doan, S. Majety, S. Grenadier, J. Li, J. Y. Lin, and H. X. Jiang, Nucl. Instrum. Methods Phys. Res., Sect. A **783**, 121 (2015).
[12]T. Sugino, K. Tanioka, S. Kawasaki, and J. Shirafuji, Jpn. J. Appl. Phys. **36**, L463 (1997).
[13]J. Li, S. Majety, R. Dahal, W. P. Zhao, J. Y. Lin, and H. X. Jiang, Appl. Phys. Lett. **101**, 171112 (2012).
[14]B. Huang, X. K. Cao, H. X. Jiang, J. Y. Lin, and S. H. Wei, Phys. Rev. B **86**, 155202 (2012).
[15]X. Z. Du, J. Li, J. Y. Lin, and H. X. Jiang, Appl. Phys. Lett. **108**, 052106 (2016).
[16]B. Arnaud, S. Lebègue, P. Rabiller, and M. Alouani, Phys. Rev. Lett. **96**, 026402 (2006).
[17]B. Arnaud, S. Lebègue, P. Rabiller, and M. Alouani, Phys. Rev. Lett. **100**, 189702 (2008).
[18]L. Wirtz, A. Marini, and A. Rubio, Phys. Rev. Lett. **96**, 126104 (2006).

[19]L. Museur, G. Brasse, A. Pierret, S. Maine, B. Attal-Tretout, F. Ducastelle, A. Loiseau, J. Barjon, K. Watanabe, T. Taniguchi, and A. Kanaev, Phys. Status Solidi RRL **5**, 214 (2011).

[20]L. Museur, E. Feldbach, and A. Kanaev, Phys. Rev. B **78**, 155204 (2008).

[21]K. Watanabe and T. Tanniguchi, Phys. Rev. B **79**, 193104 (2009).

[22]M. G. Silly, P. Jaffrennou, J. Barjon, J. S. Lauret, F. Ducastelle, A. Loiseau, E. Obraztsova, B. Attal-Tretout, and E. Rosencher, Phys. Rev. B **75**, 085205 (2007).

[23]X. K. Cao, B. Clubine, J. H. Edgar, J. Y. Lin, and H. X. Jiang, Appl. Phys. Lett. **103**, 191106 (2013).

[24]G. D. Chen, M. Smith, J. Y. Lin, H. X. Jiang, S.-H. Wei, M. Asif Khan, and C. J. Sun, Appl. Phys. Lett. **68**, 2784 (1996).

[25]K. B. Nam, J. Li, M. L. Nakarmi, J. Y. Lin, and H. X. Jiang, Appl. Phys. Lett. **82**, 1694 (2003).

[26]S. L. Rumyantsev, M. E. Levinshtein, A. D. Jackson, S. N. Mohammad, G. L. Harris, M. G. Spencer, and M. S. Shur, in *Properties of Advanced Semiconductor Materials GaN, AlN, InN, BN, SiC, SiGe*, edited by M. E.

Levinshtein, S. L. Rumyantsev, and M. S. Shur (John Wiley & Sons, Inc., New York, 2001), pp. 67–92.

[27]R. W. Lynch and H. G. Drickamer, J. Chem. Phys. **44**, 181 (1966).

[28]R. S. Pease, "An X-ray study of boron nitride," Acta Crystallographica **5**, 356 (1952).

[29]J. Serrano, A. Bosak, R. Arenal, M. Krisch, K. Watanabe, T. Taniguchi, H. Kanda, A. Rubio, and L. Wirtz, Phys. Rev. Lett. **98**, 095503 (2007).

[30]J. Wu, W.-Q. Han, W. Walukiewicz, J. W. Ager III, W. Shan, E. E. Haller, and A. Zettl, Nano Lett. **4**, 647 (2004).

[31]L. Museur and A. Kanaev, J. Appl. Phys. **103**, 103520 (2008).

[32]X. Z. Du, J. Li, J. Y. Lin, and H. X. Jiang, Appl. Phys. Lett. **106**, 021110 (2015).

[33]X. Z. Du, C. D. Frye, J. H. Edgar, J. Y. Lin, and H. X. Jiang, J. Appl. Phys. **115**, 053503 (2014).

[34]J. Li, X. K. Cao, T. B. Hoffman, J. H. Edgar, J. Y. Lin, and H. X. Jiang, Appl. Phys. Lett. **108**, 122101 (2016).

[35]D. Caruso and A. Troisi, Proc. Natl. Acad. Sci. U. S. A. **109**, 13498 (2012).